Motion Dynamics of Three-Dimensional Bodies Falling Through Water

Yonghwan Kim*[(1)], Yuming Liu[(2)] & Dick K.P. Yue[(3)]
Massachusetts Institute of Technology
Cambridge, MA 02139, USA
E-mail: ykim@vfrl.mit.edu[(1)], liu@vfrl.mit.edu[(2)], yue@mit.edu[(3)]

1. Introduction

Understanding of the dynamics of three-dimensional objects freely falling through water is of scientific interest and practical importance in naval architecture and marine engineering. The body motion is affected by environmental conditions (e.g. ambient flow and bathymetry), body geometry (e.g. body shape and mass distribution), potential flow effect (e.g. added inertia), and real fluid effect (e.g. flow separation). Accurate prediction of the body motion including all such effects is an extremely challenging task.

In this work, we focus on the study of characteristic motions of three-dimensional bodies freely falling in water. A direct numerical scheme is developed for the time-domain computation of six degree-of-freedom motions of general three-dimensional bodies dropping in water including both potential-flow and real fluid effects. The method is applied to cylindrical bodies initially released below the free surface in calm water. To adequately account for the viscous effect, we conduct laboratory experiments to measure the drag coefficients of the bodies with various body aspect ratio, end shapes and orientations to incoming flow. Depending on the initial body orientation, body aspect ratio, and mass distribution, we identify key characteristic patterns of the body motion, which compare excellently with observations in the tank-drop tests ([4,5]). The present study has a significant implication to the deployment of underwater mines and maneuvering of underwater vehicles.

2. The Equations of Motion

To describe the motion of a body, we define a space-fixed inertia (global) coordinate system (*o-xyz*) and a body-fixed (local) coordinate system (*o'-x'y'z'*), as shown in Figure 1. The equations of motion of the body can be written in the general form ([1]):

$$[E]\frac{d}{dt}\begin{Bmatrix}\vec{v}_0\\ \vec{\omega}'\end{Bmatrix}=\{q\} \tag{1}$$

where

$$[E]=\begin{bmatrix}[m]+[m_A]_{11} & [L]^T\left(-\{\vec{R}\}\times[m]+[m_A]_{12}\right)\\ \{\vec{R}\}\times[m]+[m_A]_{21} & [L]^T\left([I']-\{\vec{R}\}\times\left(\{\vec{R}\}\times[m]\right)-[m_A]_{22}\right)\end{bmatrix} \tag{2}$$

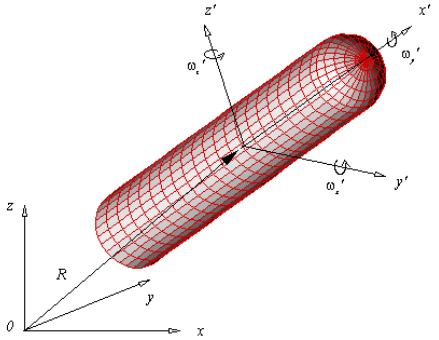

Figure 1. Coordinate System.

and

$$\{q\}=\begin{bmatrix}\{\vec{F}\}+m\left(\{\vec{v}\}\times\{\vec{\omega}\}\right)-\{\vec{v}_o\}\frac{d}{dt}[m_A]_{11}-\{\vec{\omega}\}\frac{d}{dt}[m_A]_{12}\\ \{\vec{M}\}-[L]^T\left(\{\vec{\omega}\}\times[I']\{\vec{\omega}'\}\right)+m\left(\{\vec{R}\}\times\left(\{\vec{v}\}\times\{\vec{\omega}\}\right)\right)-\{\vec{v}\}_o\frac{d}{dt}[m_A]_{21}-\{\vec{\omega}\}\frac{d}{dt}[m_A]_{22}\end{bmatrix} \tag{3}$$

where $\{\vec{v}_0\}$ and $\{\vec{\omega}'\}$ are the vectors of the translational velocity of the body frame and the angular velocity of the body in the body frame, $\{\vec{v}\}$ and $\{\vec{\omega}\}$ the vectors of the translational and rotational velocities of a point *(x, y, z)* in the global frame, *m* the body mass, $[m]$ and $[I']$ the matrices of mass and moment of inertia in the body frame, $[L]$ the transformation matrix from global frame to local frame, and $\{\vec{F}\}$ and $\{\vec{M}\}$ the vectors of the external force and

moment on the body including the gravity, buoyancy, viscous-induced drag and lift. In addition, $[m_A]$ is the added inertia matrix written as

$$[m_A]=\begin{bmatrix}[m_A]_{11} & [m_A]_{12}\\ [m_A]_{21} & [m_A]_{22}\end{bmatrix}. \tag{4}$$

3. Hydrodynamic Force and Moment on a Falling Body

The force and moment on a body falling through water contain three components respectively due to gravity, hydrostatic buoyancy, and flow-induced hydrodynamic pressure. In equations (1)~(4), the hydrodynamic component due to the potential-flow effect is taken into account in the added inertia matrices while the viscous-induced drag and moment are treated as external force $\{\vec{F}\}$ and moment $\{\vec{M}\}$. The viscous force on the body in the body frame is given by

$$\{F'\}^T=\left\{\frac{1}{2}\rho C_{D,\pm L/2}S|v_{x'}|v_{x'},\quad \frac{1}{2}\rho\int_{-L/2}^{L/2}C_{D,YZ}(x')D(x')|v_{y'}(x')|v_{y'}(x')\,dx',\quad \frac{1}{2}\rho\int_{-L/2}^{L/2}C_{D,YZ}(x')D(x')|v_{z'}(x')|v_{z'}(x')\,dx'\right\} \tag{5}$$

where L is the body length, S the frontal projection area, $D(x')$ section diameter, and $(v_{x'},v_{y'},v_{z'})$ the flow velocities. Here, $C_{D,\pm L/2}$ and $C_{D,YZ}(x')$ are the viscous drag coefficients of the body in the longitudinal and transverse directions. The moment can be computed by multiplying the moment arm to equation (5).

The drag coefficients depend on flow direction and speed, body shape, and aspect ratio. Only limited data for general bodies is available in the existing studies ([2,3]). In this study, we conduct a series of model tests to measure the drag coefficients. Four models with two different aspect ratios (L/D=3,6) and two frontal shapes (blunt and spherical) are considered in the experiment. For each model, measurements of drag/lift and moment on the body are taken with various incoming flow speeds and model orientations. Figure 2 shows two sample test models installed in water tunnel.

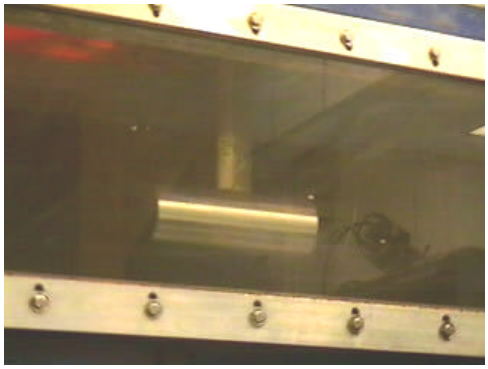

(a) L=3.5-in, D=10.5-in, blunt ends

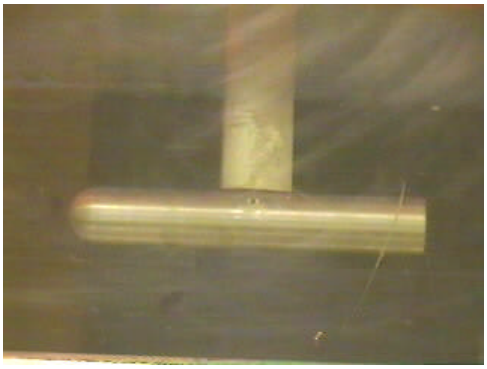

(b) L=2.0-in, D=12.0-in, spherical front end

Figure 2. Test models installed in water tunnel.

4. Solution Scheme and Results

Though a closed-form analytic solution can be derived for a few special cases, equation (1) needs to be solved numerically under general conditions. In this study, the 4-th order Runge-Kutta scheme is applied for integration of equation (1) with time. At any instant, the added inertia matrix (4) is computed using a panel method.

When the centers of mass, buoyancy, and added inertia of a body coincide, the motion of the body dropping in calm water shows a simple trajectory. In this case, an analytic solution can be obtained with the instantaneous body velocity given by

$$v_z(t) = \begin{cases} V_{T.V.} \tanh\left\{\sqrt{AB}(t+c)\right\} & \text{if } v_z(t=0) < V_{T.Z.} \\ V_{T.V.} \coth\left\{\sqrt{AB}(t+c)\right\} & \text{if } v_z(t=0) \geq V_{T.Z.} \end{cases} \tag{6}$$

where

$$V_{T.V.} = \sqrt{\frac{2(mg - \rho\ \nabla g)}{\rho C_d\ S}},\quad A = \frac{\rho\, C_{D,YZ} S}{2(m+m_A)},\quad B = \frac{mg - \rho\ \nabla g}{m+m_A},\quad c = \frac{1}{2\sqrt{AB}} \ln \left| \frac{\sqrt{B} + \sqrt{A}\, v_Z(t=0)}{\sqrt{B} - \sqrt{A}\, v_Z(t=0)} \right|, \tag{7}$$

and ∇ is the body volume. Here $V_{T.V.}$ represents the terminal velocity of the body.

Figure 3 shows the comparison of the field measurement of the vertical acceleration with the analytic prediction of (6) for a truncated horizontal circular cylinder of diameter 0.168m and length 1.01m. The field drop test was performed at a coastal bay of water depth 12.3m ([5]). It shows that the simple analytic solution agrees well with the field measurement.

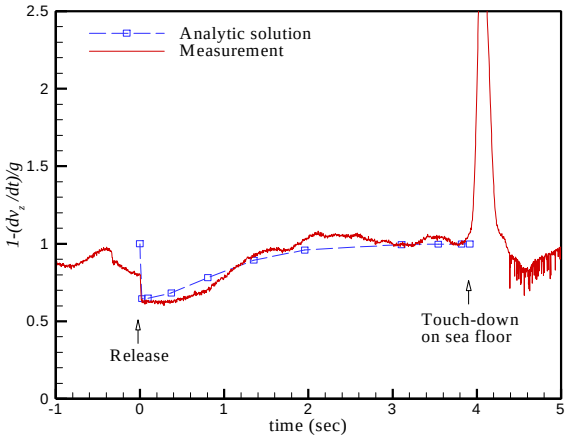

Figure 3. Comparison of the field measurement of the vertical acceleration of a cylindrical body ([5]) with the analytic solution.

When the centers of mass, buoyancy, and added inertia differ, the motion attitude becomes much more complicated. In particular, a slight variation in initial body orientation and/or flow environment (e.g. current or surface wave) can result in a large difference in the body trajectory. Figure 4 shows key representative patterns observed in the tank drop tests. The tests are conducted at the explosive pond of U.S. Naval Research Laboratory ([4]). The models used in the tank tests have the same shapes as in Figure 2 but of different sizes and mass centers.

Many numerical tests have been performed in order to cooperate the physical mechanisms with numerical modeling. It is found that the motion pattern depends significantly on initial body orientation, body aspect ratio, and mass center. Proper treatment of the viscous effects is also of importance to the prediction of body motion.

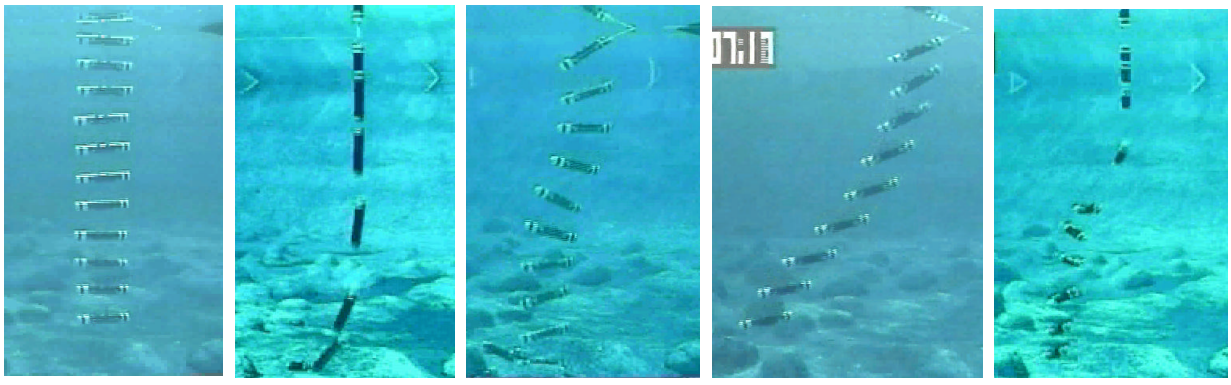

(a) (b) (c) (d) (e)

Figure 4. Representative patterns of falling body trajectory observed in tank tests ([4], edited).

Figure 5 shows our numerical predictions of the body trajectories. Figure 5a represents the case where the mass center coincides with the body geometry center. For this case, body shows a simple vertical trajectory which can simply be predicted by the analytic solution (6). Figure 5b shows a trajectory of vertical drop when a small initial disturbance is imposed in the transverse direction. A small disturbance can largely change the direction of body

motion as observed in the experiment. Figure 5c shows a seesaw-like behavior of the body motion. This is a typical pattern when the mass center is slightly deviated from the body geometry center. Figure 5d shows a different falling pattern with Figure 5c although they have the same initial drop angle. The distance between mass and volume centers in Figure 5d is slightly larger than that in Figure 5c. Figure 5e shows a combination of different patterns in Figures 5b, 5c, and 5d. The aspect ratio of the model in Figure 5e is half of the models in previous figures. In general, the motion attitude becomes more profound when the aspect ratio becomes smaller.

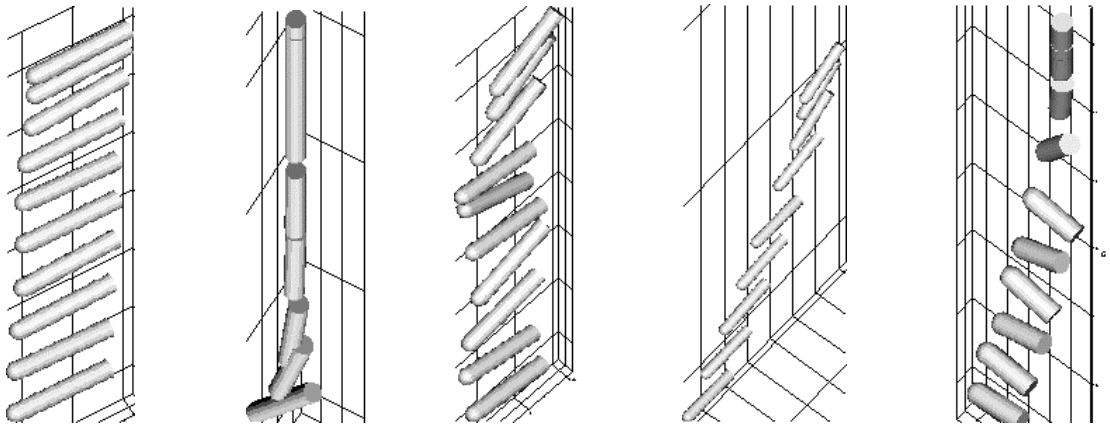

(a) (b) (c) (d) (e)

Figure 5. Numerical solutions of different motion patterns.

Figure 6 compares the trajectories of the body with different mass centers. Figure 6a is a typical motion pattern when the mass center is close to the buoyancy center. In this case, the pitch moment due to weight and buoyancy does not exceed the moment due to viscous-induced drag. However, when the mass center is far from the buoyancy center, the pitch moment can overcome the viscous-induced resistance moment. Then, the body motion can show a tumbling feature, as in Figure 6b. Such a tumbling motion is also observed in tank tests for models with small aspect ratios.

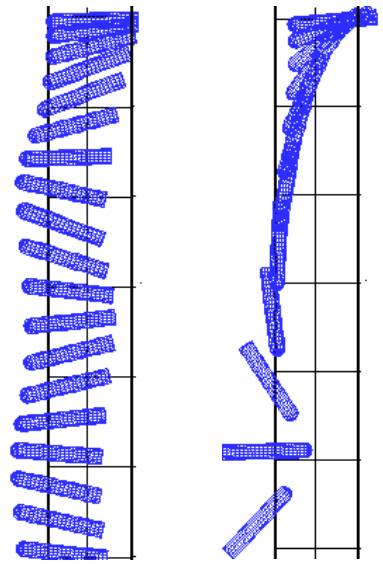

(a) (b)

Figure 7. Effect of mass center; mass center at 0.05L (a) and 0.2L (b)

Acknowledgement

This research is supported by Office of Naval Research. Both field and tank drop test data is provided by Dr. Phil Valent of Naval Research Laboratory, Stennis Space Center.

References

[1] Wierzbicki & Yue, 'Impact damage of Challenger crew compartment', MIT report, 1986.
[2] Hoerner, 'Fluid dynamics drag', Hoerner Fluid Dynamics, 1975.
[3] Williams & Vukelich, 'The USAF stability and control digital datcom', Technical report of Wright-Patterson Air Force Base, 1980.
[4] Valent & Holland, 'Quick look report, Model mine hydrodynamic tests', NRL Internal Memorandum, 2001.
[5] Valent, 'Transmittal of 2-4 Nov. 2000 mine drop data', NRL Internal Memorandum, 2001.

17th IWWWFB

Discussion Sheet

Abstract Title :	Motion Dynamics of Three-Dimensional Bodies Falling Through Water		
(Or) Proceedings Paper No. :	21	***Page :***	081
First Author :	Kim, Y., Liu, Y. and Yue, D.K.P.		
Discusser :	Rod C.T. Rainey		

Questions / Comments :

This problem has been extensively studied by the offshore oil industry. Typically, a slender body (e.g. a length of drill string) is dropped end-on into the water, and it is necessary to ensure that it deviates sufficiently as it drops to avoid hitting something valuable on the seabed (e.g. a wellhead).
There is a complete formulation of all the slender-body potential-flow forces in my 1995 Proc. Roy. Soc. Paper (A450 pp391-416). In the special case where there are no waves, these potential-flow forces give the "rocking" and "tumbling" trajectories shown at the end of the author's paper. Those trajectories are described by exact formulae (Art.127 of Lamb's text book), which serve as a valuable cross-check on any computer code – I am surprised that the authors do not cite them.

Author's Reply :
(If Available)

Author did not respond.